

June 2022

Engineering and Evaluation of Reconstituted HDL Nanoparticles to Target Tumor-Associated Macrophages.

Aishwarya Menon
University of Massachusetts Amherst

Follow this and additional works at: https://scholarworks.umass.edu/masters_theses_2

Recommended Citation

Menon, Aishwarya, "Engineering and Evaluation of Reconstituted HDL Nanoparticles to Target Tumor-Associated Macrophages." (2022). *Masters Theses*. 1204.
<https://doi.org/10.7275/28269836> https://scholarworks.umass.edu/masters_theses_2/1204

This Open Access Thesis is brought to you for free and open access by the Dissertations and Theses at ScholarWorks@UMass Amherst. It has been accepted for inclusion in Masters Theses by an authorized administrator of ScholarWorks@UMass Amherst. For more information, please contact scholarworks@library.umass.edu.

**Engineering and Evaluation of Reconstituted HDL Nanoparticles to
Target Tumor-Associated Macrophages.**

A Thesis Presented

by

Aishwarya Vinod Menon

Submitted to the Graduate School of the
University of Massachusetts Amherst in partial fulfillment
of the requirements for the degree of

Master of Science in Chemical Engineering

May 2022

Chemical Engineering

© Copyright 2022
Aishwarya Menon All Rights Reserved

Engineering and Evaluation of Reconstituted HDL nanoparticles to target Tumor-Associated Macrophages.

A Thesis Presented

by

Aishwarya Menon (amenon@umass.edu)

Department of Chemical Engineering
University of Massachusetts Amherst

Approved as to style and content by:

Ashish Kulkarni, Chair

Jessica Schiffman, Member

Peter Beltramo, Member

Jessica Schiffman, Department Head

Department of Chemical Engineering

ACKNOWLEDGEMENTS

I would like to thank my advisor Prof. Ashish Kulkarni for his patience and guidance throughout this project. I would also like to thank my committee members Profs. Jessica Schiffman and Peter Beltramo for their valuable inputs.

I would like to take this opportunity to thank my lab members Anthony, Anh, Anujan, Dipika, James and Vaishali. Thank you for your help, patience, and companionship.

Lastly, I would like to thank my parents for their constant love and support.

ABSTRACT

Engineering and Evaluation of Reconstituted HDL nanoparticles to target Tumor-Associated Macrophages.

MAY 2022

AISHWARYA MENON,

B.TECH., INSTITUTE OF CHEMICAL TECHNOLOGY

M.S.ChE., UNIVERSITY OF MASSACHUSETTS AMHERST

Directed by: Ashish Kulkarni

Conventional cancer therapies such as chemotherapy and radiation often lead to severe side effects since they are unable to specifically target the tumor. Additionally, they do not guarantee the prevention of metastasis or recurrence. Recent developments on small-molecule inhibitors, such as kinase inhibitors that target cellular pathways characteristically upregulated in cancer cells, show promise. However, significant challenges such as tolerance and mutations causing drug resistance need to be overcome. Immunotherapy, wherein the host's immune system is leveraged to recognize and target cancer cells, is a better alternative that shows reduced toxicity. Macrophages are an attractive target for immunotherapy seeing as they constitute 50% of the infiltrating leukocytes in the tumor microenvironment. Their plastic nature allows them to be modulated from pro-tumor to anti-tumor phenotype. Although, it does not work for everyone, necessitating a need to monitor response to medication at earlier time points.

In this thesis, I have designed an HDL mimicking nanoparticle system to target tumor associated M2 macrophages through the SRB1 receptor. The nanoparticle was optimized for better stability, better loading of the targeting peptide, and the drug as well. It was used to deliver a CSF1R inhibitor drug to successfully repolarize pro-tumor M2 macrophages to anti-tumor M1 phenotype. In addition to that, it was also used to deliver an Arginase-responsive probe that only fluoresces when engulfed by arginase-producing M2 macrophages, differentiating them from arginase non-producing M1 phenotype. Through this study, the SRB1 receptor was successfully targeted to effectively deliver small molecules. This can be used to target and modulate tumor-associated macrophages.

CONTENTS

ACKNOWLEDGEMENTS	iv
ABSTRACT	v
LIST OF TABLES	ix
LIST OF FIGURES	x
CHAPTER I	1
1.1 Motivation	1
1.2 Role of the Immune System in Cancer	2
1.3 Literature Survey	4
1.4 Research Objectives	6
CHAPTER 2	9
2.1 Materials	9
2.2 Methods	9
2.2.1 Peptide synthesis and Characterization	9
2.2.2 Nanoparticle Synthesis and Characterization	10
2.2.3 Flow Cytometry Protocol for SRB1 staining	10
2.2.4 Internalization	11
2.2.5 Repolarization	11
2.2.6 Microscopy	11
CHAPTER 3	12

3.1 R4F Peptide Synthesis	12
3.2 Synthesis of HDL Nanoparticle	12
3.3 Optimization of Peptide Loading.....	13
3.4 Optimization for Stability	14
3.5 Optimization of Encapsulation Efficiency	15
Chapter 4	16
4.1 SRB1 Expression on M2 and M1 Polarized Macrophages.....	16
4.2 Internalization of HDL Nanoparticles in M2 polarized RAW264.7 Macrophages..	17
4.3 Repolarization of M2 polarized RAW264.7 Macrophages by BLZ-Chol loaded HDL Nanoparticle.....	17
4.4 Validation Assay with Arginase-Responsive Probe Loaded HDL Nanoparticle.....	18
CHAPTER 5	20
BIBLIOGRAPHY	21

LIST OF TABLES

Table 1: Optimization of Peptide Loading	14
--	----

LIST OF FIGURES

Figure 1: Estimated statistics for new cancer cases and deaths in the United States in 2021, Cancer Therapy Advisor, 2021	2
Figure 2: Anti-tumor and Pro-tumor functions associated with TAMs, Anfrey et al, 2019	4
Figure 3: Schematic to deliver CSF1R inhibiting drug to M2 macrophages.....	7
Figure 4: Schematic for delivering Arginase responsive probe to M2 macrophages	8
Figure 5: MALDI-TOF analysis of R4F	12
Figure 6: Variation in Size due to changes in peptide composition.....	13
Figure 7: Changes in hydrodynamic diameter over three days in nanoparticles with different cholesterol compositions.....	14
Figure 8: BLZ-Chol loaded HDL Nanoparticle with size ~ 18 nm	15
Figure 9: SRB1 expression as percentage when compared to positive control.....	16
Figure 10: Internalization of FITC loaded HDL nanoparticle over 24 hours.....	17
Figure 11: Repolarization of M2 RAW264.7 Macrophages with BLZ-Chol loaded HDL nanoparticles. Free BLZ-Chol was used as control.....	18
Figure 12: Comparison of Probe fluorescence between M1 and M2 polarized Macrophages	19

CHAPTER I

INTRODUCTION

1.1 Motivation

According to the WHO, cancer is listed as one of the leading causes of premature death. The American Cancer Society projects 1.93 million new cases and over 600,000 deaths related to cancer in 2021. Cancers of the prostate, breast, lung, and colon are expected to be the most common (**FIG 1**). The most common factor contributing to cancer deaths is metastasis, which is when the primary tumor spreads to other organs and body parts. [12].

Conventional treatments for cancer, including radiation, chemotherapy, and surgery, often lead to severe side effects. Both radiation and chemotherapy, though possessing high tumoricidal capacity, do not specifically target cancers. Therefore, they tend to be severely toxic to other cells and organs. Side effects can range from hair loss, nausea, diarrhea to heart failure, central nervous system toxicities, hypertension etc. [1] Surgery is only possible depending upon the accessibility of the cancerous mass and does not guarantee prevention of metastasis or recurrence. [2]

Targeted therapies, on the other hand, target cellular pathways that are characteristic of cancer cells, thereby leaving healthy cells unharmed. Small molecule inhibitors such as kinase inhibitor imatinib [3], EGFR inhibitor Gefitinib [4] etc. and antibodies such as VEGF targeting Bevacizumab [5] are some examples of FDA approved targeted treatments. However, there are several challenges that need to be overcome such as mutations leading drug resistance and tolerance. [6]

It has been well observed that the immune system plays a critical role in suppressing or promoting tumors. [7] Several immune check point inhibitors such as anti CTLA-4 drug ipilimumab [8] and anti PD/PDL1 drug pembrolizumab [9] have been approved by the FDA against advanced melanoma, non-small cell lung cancer, renal cell carcinoma and Hodgkin’s lymphoma. However, while immunotherapy is an attractive option, not all patients respond equally to it. Currently, only 20% to 40% of recipients respond positively [10]. Moreover, conventional imaging techniques like PET lack the sensitivity and specificity for early response assessment. [11] Therefore, there is a need to have an imaging system that can detect early response to therapies to better predict its efficacy.

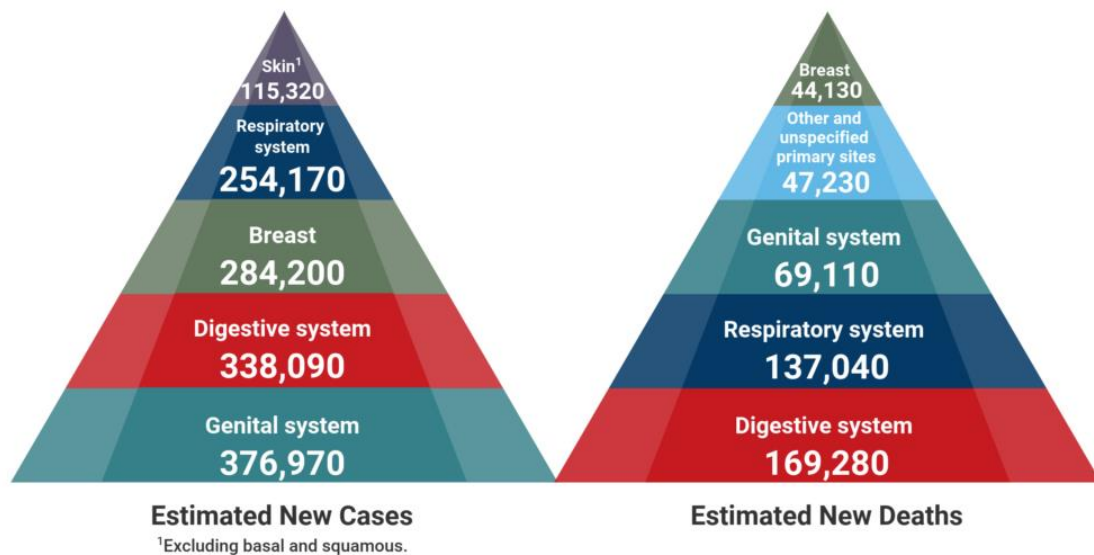


Figure 1: Estimated statistics for new cancer cases and deaths in the United States in 2021, Cancer Therapy Advisor, 2021

1.2 Role of the Immune System in Cancer

A growing solid tumor acquires several biological characteristics that allow it to grow unhindered. They hijack cell regulation signals through mutations or inhibition of suppressors and proliferate endlessly. [13] Angiogenesis, or the process of sprouting new

blood vessels from existing ones, ensures they have a supply of nutrients and oxygen, as well as channel to dispose of metabolic wastes and carbon dioxide. [14] Mutations leading to loss of adhesion molecules such as E-cadherin allows them to invade and spread to distant organs. [15] Additionally, they escape recognition by immune cells by upregulating expression of markers such as CD 47, PD L1 etc. that prevent the immune cells from killing them. [16]

They do not achieve this alone but are helped by stromal cells that are recruited into the tumor, which include immune cells. Macrophages are a major component among them. In this context, they are referred to as Tumor-Associated Macrophages or TAMs. Macrophages can change their phenotype in response to chemical messengers called cytokines that are released by tumor and stromal cells. [17] In the presence of TLR agonists such as LPS and cytokines such as $\text{INF } \gamma$, macrophages get activated to a pro-inflammatory phenotype known as the classically activated 'M1' state, characterized by an upregulation of CD80 and CD86 surface markers. M1 activated macrophages have enhanced phagocytosis, antigen presentation capability and tumoricidal activity. They also secrete several pro-inflammatory cytokines such $\text{TNF-}\alpha$, IL-6, IL-12 and IL-23 that aid in the activation of effector cytotoxic T cells. Alternatively, in the presence of IL-4 and IL-13, macrophages get polarized to an 'M2' state with increasing levels of CD206 surface markers. M2 macrophages are usually associated with wound healing, immune suppression, and anti-inflammatory responses. [18]

TAMs are often associated with worse prognosis. This is because cytokines present in the tumor microenvironment activate macrophages into M2 state. These M2 TAMs support angiogenesis, tumor cell metastasis and protect the tumor from immune response through

secretion of VEGF A, TGF β and through T-cell check point blockage which helps cancers escape immune surveillance. (Fig 2) [19,20] They also secrete arginase 1 (ARG 1) that inhibit T cell activity by hydrolyzing L-arginine and converting it into urea and L-ornithine. It is also implicated in angiogenesis and anti-inflammatory properties.

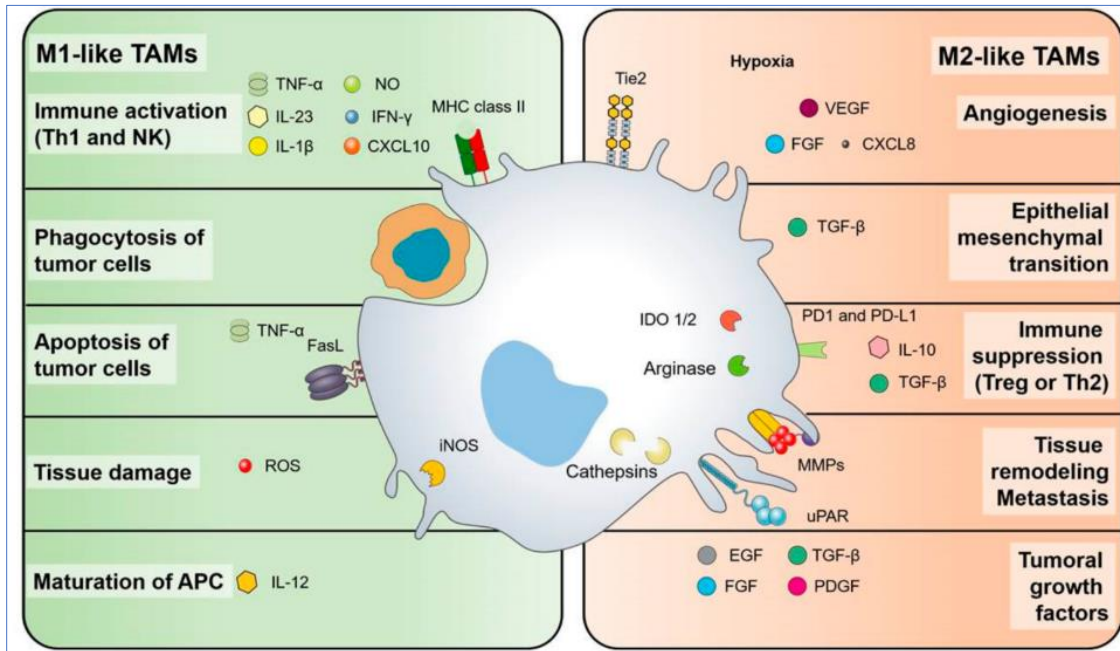


Figure 2: Anti-tumor and Pro-tumor functions associated with TAMs, Anfrey et al, 2019

1.3 Literature Survey

To utilize TAMs as an effective immunotherapy target, previous efforts have been made to prevent recruitment of macrophage into the tumor through disruption of the CCL2-CCL2 [21] receptor and CXCL12-CXCL receptor 4 axes. [22] While pre-clinical studies found that this strategy helped eradicate tumor, discontinuing the treatment led to rebounds. [23] Efforts have also been made to target and deplete M2 TAMs through use of bisphosphonates such as zoledronate and clodronate. However, there is a strong possibility that immune-protective cells are also targeted and eliminated, leading to

severe repercussion such as bacterial infections. [24] **FIG 3** summarizes the principal strategies of utilizing TAMs for anti-cancer therapy.

Due to their plastic nature, macrophages can change their phenotype in response to change in the microenvironment they are in. This has led to efforts in ‘re-educating’ TAMs from pro-tumoral M2 phenotype to anti-tumoral M1 phenotype through multiple pathways such as CSF1/CSF1R blockage, TLR agonists, PI3K γ and CD40 agonists. Cancer cells secrete Macrophage Colony Stimulating Factor (MCSF) which binds to its receptor CSF1R on macrophages. [25] This in turn activates a cascade of downstream signaling resulting in their polarization to M2 phenotype. Blocking of the CSF1R can be achieved through small molecules drugs such as BLZ945, PLX3397, ARRY 382 etc. Blocking of CSF1R by BLZ945 has successfully resulted in repolarization of M2 macrophages into M1 type, leading to anti-tumor response and tumor regression. [26] Therefore, targeted delivery of BLZ945 to M2 TAMs is an attractive avenue to pursue.

With many aggressive cancers, such as breast cancers, early detection of tumor progression and metastasis becomes critical. Conventional imaging techniques such as CT, PET and MRI lack the sensitivity required for this. [] Also, several patients undergoing immunotherapy face severe side effects due to over-activation of the immune system such as hepatic autoimmunity. [28] Every patient responds differently, making it difficult to use standardized tests and imaging techniques. Therefore, there is a need for a system that can accurately monitor early tumor response to therapy to differentiate between responders and non-responders. Since M2 TAMs are heavily linked with metastasis and overall poor prognosis, they can be used as diagnostic marker to predict early stages of metastasis and to monitor patient response.

1.4 Research Objectives

I aim to design and evaluate a synthetic nanoparticle system that can deliver therapeutic or diagnostic agents to M2 TAMs. To target TAMs with this system, I intend to target the Scavenger Receptor B Class1 (SRB1) receptor, a murine multiligand cholesterol receptor expressed on hepatic cells, smooth muscle cells, endothelial cells, and macrophages as well. It promotes the uptake of cholesterol through High Density Lipoprotein (HDL), a lipoprotein made by the liver. HDL consists mostly of phospholipids, cholesterol and Apolipoproteins with a hydrophobic core encapsulating triglycerides and esterified cholesterol. [29] The Apolipoprotein A1 is responsible for the interaction of HDL with SRB1, leading to uptake of the cargo through a process called selective lipid uptake in which only the encapsulated cargo is delivered. [30] This ability of SRB1 to selectively uptake hydrophobic molecules, bypassing lysosomal degradation makes it an attractive gateway for delivery of small molecules reconstituted in HDL nanoparticles. []

Previously, SRB1 receptor has been targeted through synthetic or reconstituted HDL nanoparticles in atherosclerosis and tumor disease models. [31, 32] Advantages of using HDL nanoparticles include their relatively small size (~20nm), non-toxicity and biodegradability. Human plasma derived Apo A1 has been used to synthesize HDL along with phospholipids such as DPPC, DOPC etc., although recently several non-homologous mimetic peptides have also been shown to target SRB1. [33] These nanoparticles have been used to deliver anticancer drugs and imaging agents to tumors that overexpress SRB1. However, very little research has been done towards using synthetic HDL

particles to target and repolarize M2 TAMs in tumor models or in using them as predictive markers for imaging.

In this project, I have designed an HDL nanoparticle system with the aim to deliver the repolarizing agent BLZ-945 to M2 macrophages via the SRB1 receptor. **(FIG 3)** Additionally, I have also used this system to deliver an arginase 1-responsive probe that can differentiate between M1 and M2 macrophages. **(Fig 4)** The probe has a peptide backbone to which a dye is attached. A quencher is attached to the arginine molecule in the peptide backbone. Upon internalization, Arginase 1, produced only in M2 macrophages, is expected to cleave the bond between arginine and quencher, causing the dye to fluoresce. This will allow M2 macrophages to be selectively imaged.

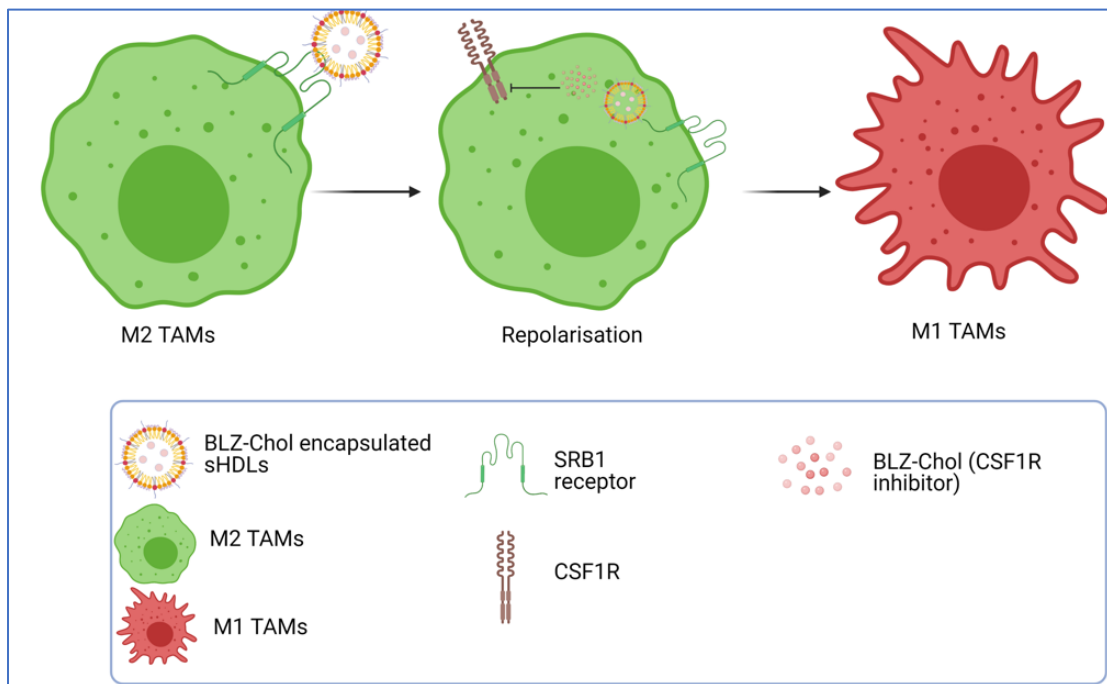


Figure 3: Schematic to deliver CSF1R inhibiting drug to M2 macrophages

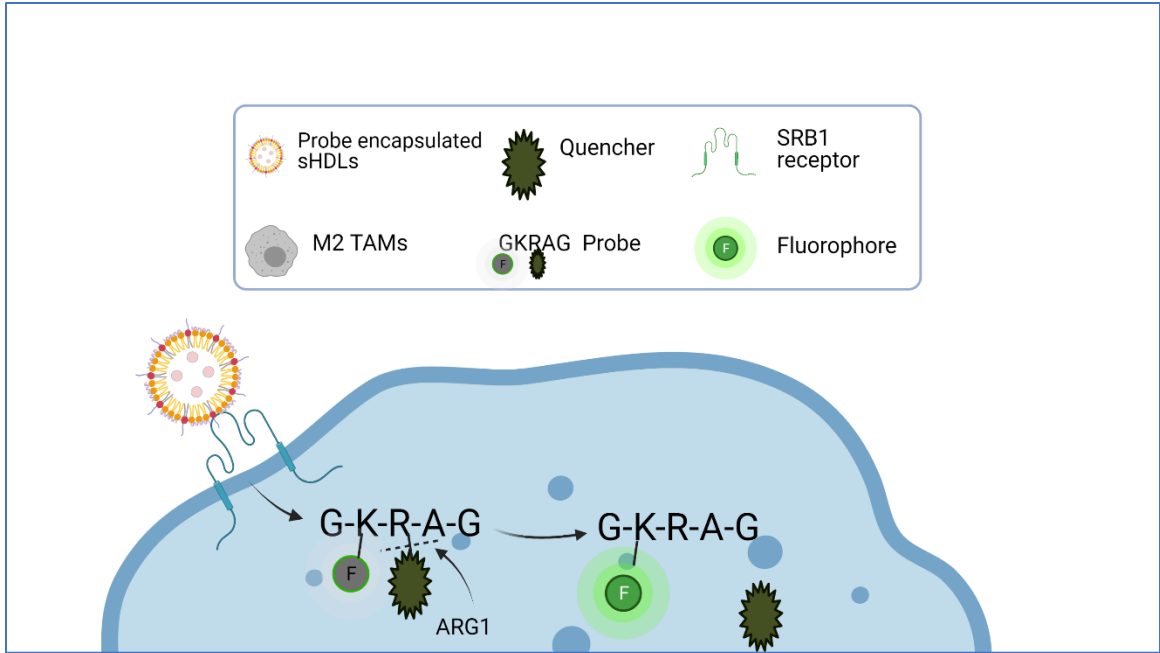


Figure 4: Schematic for delivering Arginase responsive probe to M2 macrophages

CHAPTER 2

MATERIALS AND METHODS

2.1 Materials

Dichloromethane (DCM) and N, N-dimethylformamide (DMF) were purchased from Fisher Scientific. 1,2 Dipalmitoyl-sn-glycero-3-phosphocholine (DPPC), 1,2-distearoyl-sn-glycero-3-phosphoethanolamine-N- [amine (polyethylene glycol)-2000] (ammonium salt) (DSPE-PEG amine 2000), cholesterol, and the mini handheld extruder kit (including 0.4 μm and 0.2 μm Whatman Nucleopore Track-Etch Membrane, Whatman filter supports, and 1 mL Hamiltonian syringes) were brought from Avanti Polar Lipids. BLZ-945 drug was purchased from Selleck Chem. CD16/32 (Fc-block), CD80, CD206 and SRB1 FACS antibodies were purchased from Biolegend Inc.

2.2 Methods

2.2.1 Peptide synthesis and Characterization

The R4F peptide Ac-FAEKFKKEAVKDYFAKFWD was synthesized using the AAPTEC Eclipse Peptide sequencer. The synthesized peptide was cleaved from the peptide-resin by reacting it with Reagent K, a cleavage cocktail consisting of (v/v) 82.5% TFA, 5% Phenol, 5% Thioanisole, 2.5% DODT and 5% water. The peptide was precipitated out of the resultant solution by adding it to three times the volume of ice-cold Di-ethyl Ether. The precipitate was collected upon centrifugation and further washed with Diethyl Ether three more times. The precipitate was then lyophilized and characterized using UltrafleXtreme MALDI-TOF/TOF in linear negative ion mode using α -cyano matrix.

2.2.2 Nanoparticle Synthesis and Characterization

The nanoparticle is synthesized using the thin-film hydration method. Briefly, lipids taken in various molar ratios are dissolved in 1ml of DCM in a round bottom flask. The solvent is then evaporated to form a thin film which is then rehydrated with R4F peptide dissolved in PBS at 60°C for 2 hours to form self-assembling nanoparticles. The nanoparticle is extruded through 0.2 µm and 0.05 µm polycarbonate membrane using a mini extruder. It is then passed through Sephadex G25 column. The hydrodynamic diameter was measured by Dynamic Light Scattering (DLS) using Malvern Zetasizer Nano ZSP (Malvern, UK). 10 µL of the nanoparticle solution was diluted into 1 mL using Milli-Q water and 3 sets of 10 measurements were each performed at a 90-degree scattering angle to get the mean particle size. Peptide and BLZ-945 loading are quantified by measuring absorbance using UV-VIS spectrophotometer. Fluorescein Isothiocyanate (FITC) and arginase responsive probe loading are quantified by measuring fluorescence using microplate reader.

2.2.3 Flow Cytometry Protocol for SRB1 staining

RAW264.7 cells were seeded at a density of 2×10^5 cells per well in a 12 well plate. The cells were incubated with 20ng/ml of IL4 for 24 hours to polarize them to M2 phenotype. Cells were then collected and permeabilized using Cytotfix / Cytoperm (BD biosciences) buffer as per manufacturer's protocol. Cells were then stained with anti-SRB1 antibody and analyzed using a Novocyte flow cytometer (Acea Biosciences) and the results were processed using NovoExpress 1.2.5. The cells were gated for a live population and isolated singlets to reduce autofluorescence from doublets

2.2.4 Internalization

RAW264.7 macrophages were seeded at a density of 1.5×10^6 per well in 12 well plates and were allowed to reach sub confluency. The cells were then stimulated with 20ng/ml of recombinant mouse IL-4 in DMEM media for 24 hours. Post that, the cells were treated with 5uM of FITC loaded HDL nanoparticles at 1-, 4-, 8- and 24-hours' time points. Following treatment, the cells were washed with PBS and quantified using Novocyte flow cytometer (Acea Biosciences) and the results were analyzed using NovoExpress 1.2.5.

2.2.5 Repolarization

RAW264.7 macrophages were seeded at a density of 1.2×10^6 cells per well in 12 well plates. After reaching sub-confluency, the cells were polarized to M2 phenotype by incubating them with 20nm/ml of IL-4 for 24 hours. They were then incubated with 1uM, 500nM and 100nM of BLZ945-chol or BLZ-chol loaded HDL nanoparticle for 48 hours. After 48 hours, the cells were washed and stained with Pac Blue CD80 (M1 marker) and quantified using Novocyte flow cytometer.

2.2.6 Microscopy

RAW264.7 cells were seeded at a density of 1×10^5 cells per well in an 8-chamber slide and were allowed to reach sub confluency. They were then incubated for 24 hours with 20ng/ml of IL-4 or 100ng/ml LPS and 20ng/ml IFN- γ to polarize them into M2 or M1 phenotype respectfully. They were then incubated with 1uM, 500nM and 100nM of arginase probe loaded HDL nanoparticle for 8 hours. The cells were then fixed with 4% PFA and finally stained with DAPI. Images were taken with Nikon A1R-SIME confocal microscope and were analyzed using NIS Elements 4.6

CHAPTER 3

Synthesis and Optimization of HDL Nanoparticle

3.1 R4F Peptide Synthesis

The R4F peptide was synthesized using ECLIPSE peptide sequencer and characterized using MALDI-TOF. It was found to have a molecular weight of 2315 g/mol, as was calculated theoretically. (FIG 5)

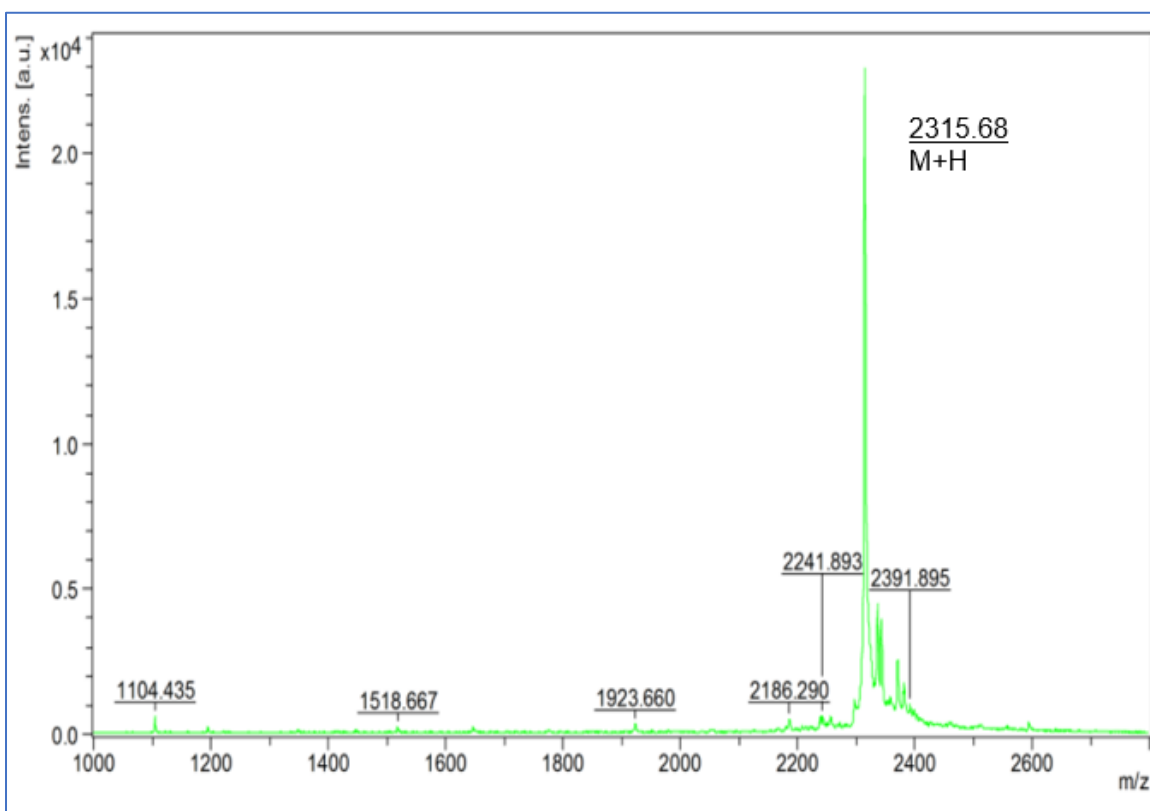


Figure 5: MALDI-TOF analysis of R4F

3.2 Synthesis of HDL Nanoparticle

HDL nanoparticle was synthesized using the thin film hydration method with different molar concentration of R4F peptide as shown in Fig 6. It was seen that at lower

molar concentration of peptide, larger sized particles were formed. This could be because the presence of peptide forms a nucleation site for the nanoparticle to form. Therefore, higher amount of peptide led to formation of smaller nanoparticles. A minimum of 10 mol percent of R4F peptide was required to make nanoparticles of 18 nm – 25 nm. From here on, further optimizations use 10 mol percent of R4F peptide.

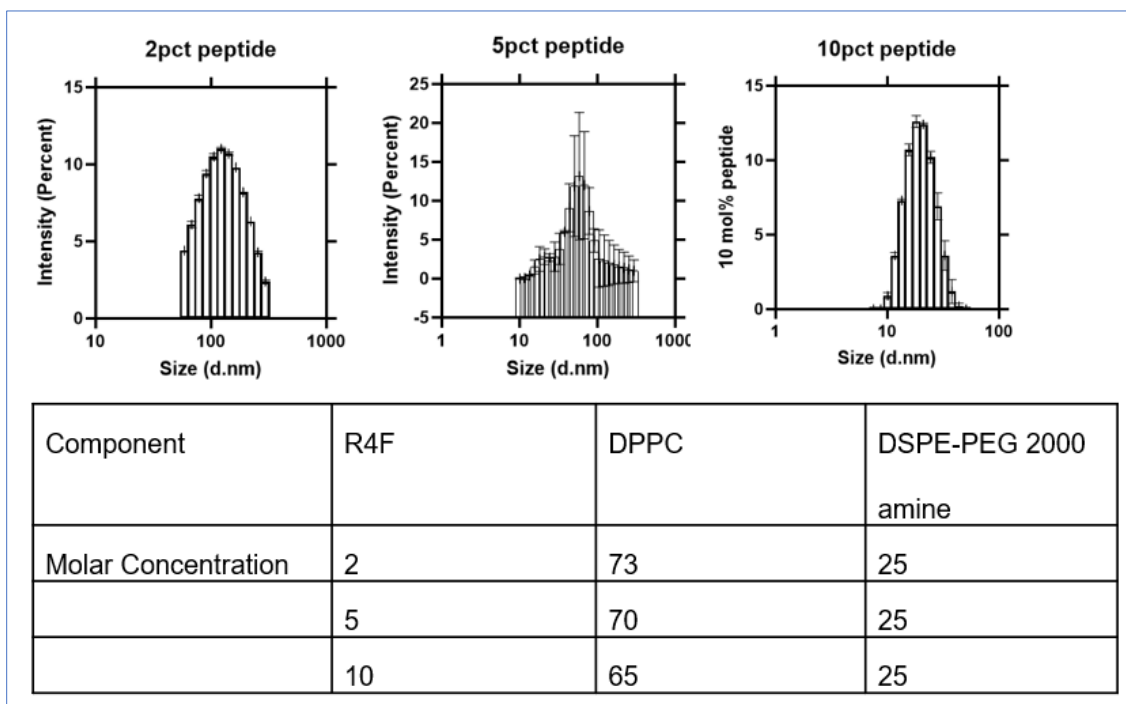


Figure 6: Variation in Size due to changes in peptide composition

3.3 Optimization of Peptide Loading

Next, to maximize the peptide loading, the mol percent of DSPE-PEG amine 2000 was reduced. This is because DSPE-PEG is known to be integrated into the nanoparticle in such a way that the PEG chains face outwards. So, reducing the content of DSPE-PEG might provide more area for the peptide to interact. The loading of the peptide, as measured by UV absorbance, was found to increase to some extent with decrease in

DSPE-PEG amine 2000. (**Table 1**) Further decrease caused instability in the HDL nanoparticle. Hence, 10 mol percent of DSPE-PEG amine 2000 was used for further experiments.

Table 1: Optimization of Peptide Loading

DSPE-PEG amine 2000	Peptide concentration
25	13%
10	40%
0	HDL nanoparticle not stable

3.4 Optimization for Stability

To increase the stability of the nanoparticle, different molar concentrations of cholesterol were added. As seen in FIG 6, adding 1 percent of cholesterol did not prevent increase in size. Increasing cholesterol content from 1 to 5% showed an increase in size stability (**FIG 7**). Increasing the cholesterol content to 10% resulted in unstable nanoparticle formation.

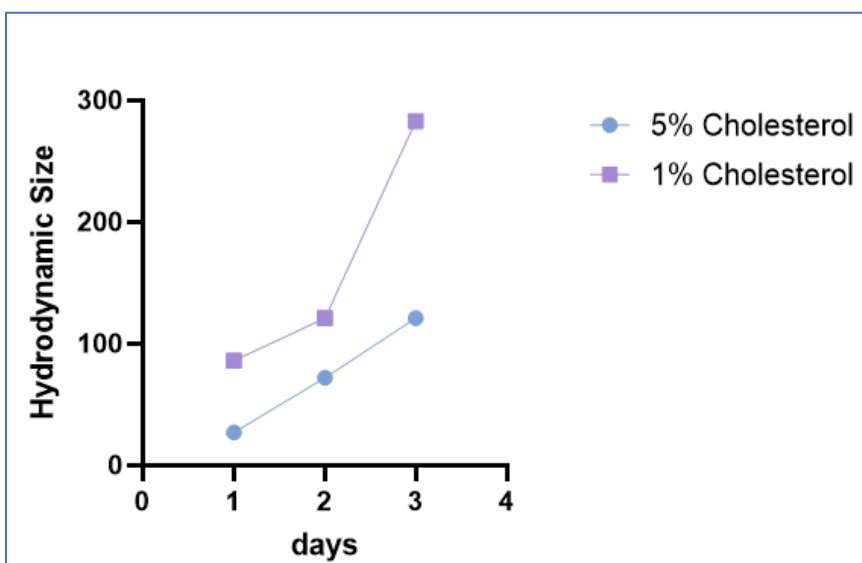


Figure 7: Changes in hydrodynamic diameter over three days in nanoparticles with different cholesterol compositions

3.5 Optimization of Encapsulation Efficiency

Finally, the CSF1R inhibitor drug was added. **(Fig 8)** The encapsulation efficiency was found to be 40%. Since the R4F peptide and BLZ-Chol have similar wavelengths of absorption for UV, DCM-water mixture was used to separate the polar and water-soluble peptide from the hydrophobic drug. The UV absorption of the separated fractions were used to calculate loading. Increasing the amount of drug was found to have no impact on the encapsulation efficiency. This could be because of the relatively small size of the particle (~ 18 nm).

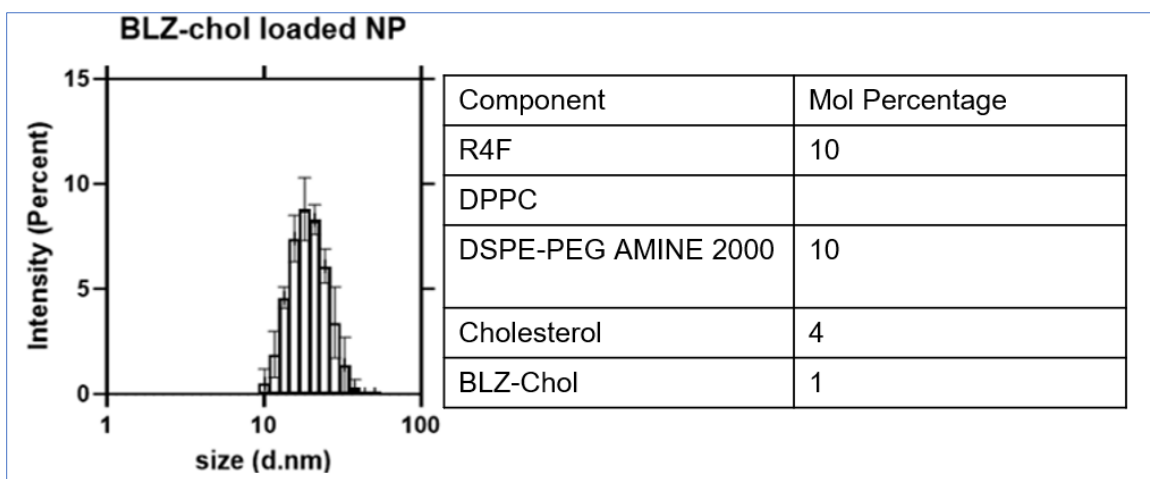


Figure 8: BLZ-Chol loaded HDL Nanoparticle with size ~ 18 nm

Chapter 4

DELIVERY OF THERAPEUTIC AND DIAGNOSTIC AGENT USING HDL NANOPARTICLES

4.1 SRB1 Expression on M2 and M1 Polarized Macrophages

To study the expression of SRB1 receptor on M2 and M1 polarized RAW264.7 macrophages, they were permeabilized and stained with anti-SRB1 antibody. 4T1 cancer cells were used as a positive control, as they are known to express SRB1. While permeabilizing and fixing macrophages, it was seen that they stuck together. This made it difficult to gate for singlet population to rule out autofluorescence. To counter this, the acquiring buffer needed to be optimized to include 1% EDTA to

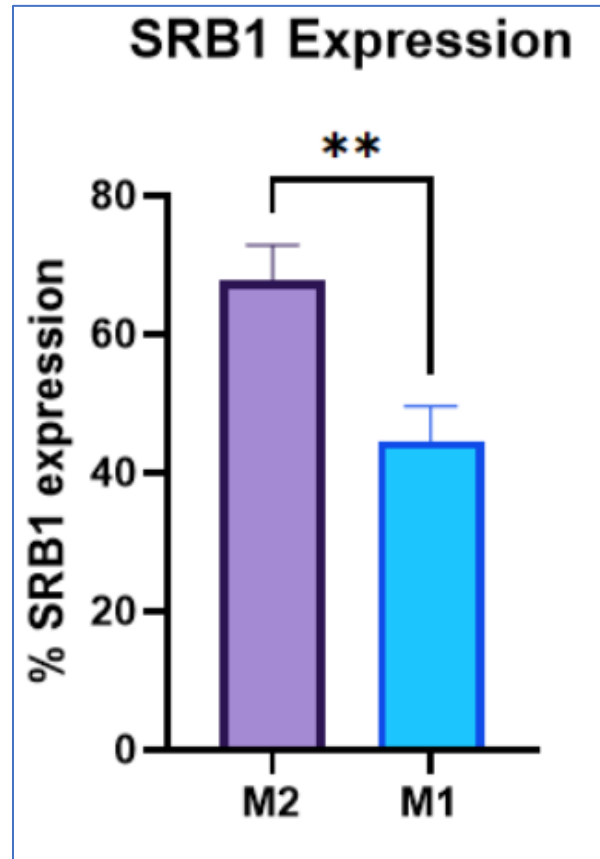


Figure 9: SRB1 expression as percentage when compared to positive control

prevent the cells from sticking together. It was seen that M2 polarized macrophages express SRB1 significantly more than M1 polarized macrophages. Therefore, M2 macrophages can be selectively targeted through the SRB1 receptor. (FIG 9)

4.2 Internalization of HDL Nanoparticles in M2 polarized RAW264.7 Macrophages

FITC loaded nanoparticle was used to study the internalization in M2 polarized RAW264.7 macrophages. The major concern here was the small size of nanoparticle. While macrophages are known to indiscriminately phagocytose particles over 100 nm in size, it has been shown that particles smaller than 100nm are

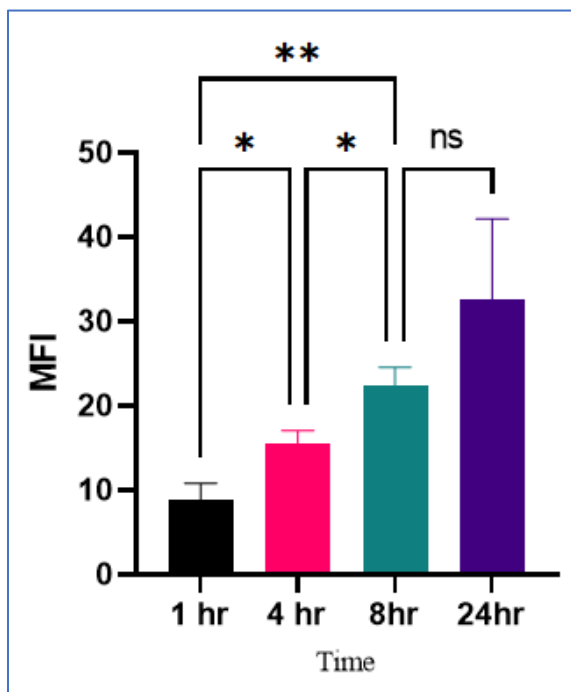


Figure 10: Internalization of FITC loaded HDL nanoparticle over 24 hours

not readily phagocytosed. [] While just the nanoparticle without the targeting

peptide would have been the ideal control, we found that it was more than 150 nm in size. This difference in size between the control and HDL nanoparticle might influence its internalization, therefore free dye was used as control. The FITC loaded nanoparticles were seen to be more readily internalized than the free dye control and maximum internalization was observed at 8 hours' time point (FIG 10).

4.3 Repolarization of M2 polarized RAW264.7 Macrophages by BLZ-Chol loaded HDL Nanoparticle

BLZ-Chol loaded HDL nanoparticles were added to M2 polarized RAW264.7 macrophages to repolarize them to M1 phenotype. Free drug was used as control. Of the three concentrations used, 1uM showed considerable increase in the expression of M1

marker CD80. **(FIG 11)** The concentrations were calculated based on BLZ-Chol loading in the HDL nanoparticles.

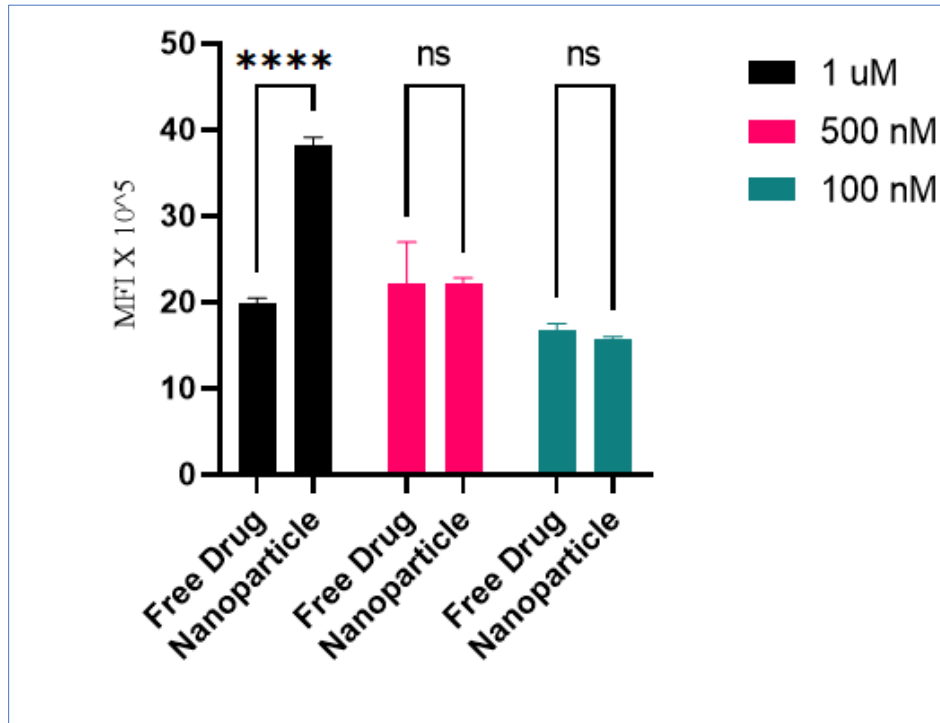


Figure 11: Repolarization of M2 RAW264.7 Macrophages with BLZ-Chol loaded HDL nanoparticles. Free BLZ-Chol was used as control

4.4 Validation Assay with Arginase-Responsive Probe Loaded HDL Nanoparticle

Arginase responsive probe was loaded into the HDL nanoparticle with an encapsulation efficiency of 30%. Upon testing it on M2 and M1 macrophages, it was found that, at 100nM concentration, only M2 macrophages show fluorescence. **(Fig 12)** At higher concentrations, the system was found to be toxic to the cells.

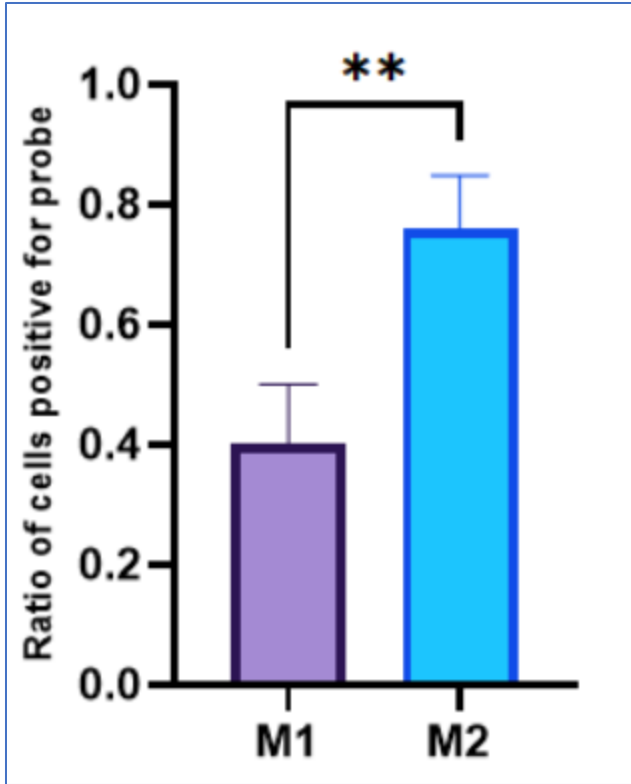


Figure 12: Comparison of Probe fluorescence between M1 and M2 polarized Macrophages

CHAPTER 5

DISCUSSION

In this project, an SRB1 targeting HDL nanoparticle system was designed to deliver agents to M2 polarized macrophages. Several aspects of the nanoparticle, such as size, peptide loading, and drug loading were optimized. After validating the expression levels of SRB1 on macrophages, internalization studies showed that the nanoparticles get internalized within 8 hours. It was then used to deliver CSF1R inhibitor drug BLZ-945, a repolarizing agent, to M2 macrophages. An increase in M1 marker CD80 was seen after a 48-hour incubation period with 1 μ M of BLZ-Chol loaded HDL nanoparticle. This increase was significantly more than compared to free drug. It was also used to deliver an arginase-responsive probe to both M1 and M2 polarized macrophages. M2 macrophages showed significantly high fluorescence as compared to M1 macrophages, even treated with a concentration as low as 100nM. This shows that the system can effectively target SRB1 expressing M2 macrophages. It can be used to target M2 like macrophages in many disease models, particularly TAMs in tumors. Future work could be directed towards validating the system in in-vivo tumor models for both therapeutic and diagnostic purposes.

BIBLIOGRAPHY

1. Toale K.M., Johnson T.N., Ma M.Q. (2016) Chemotherapy-Induced Toxicities. In: Todd K., Thomas, Jr. C. (eds) *Oncologic Emergency Medicine*. Springer, Cham.
2. Jiang, W., Von Roemeling, C.A., Chen, Y., Qie, Y., Liu, X., Chen, J. and Kim, B.Y., 2017. Designing nanomedicine for immuno-oncology. *Nature Biomedical Engineering*, 1(2), pp.1-11.
3. Sawyers CL. Opportunities and challenges in the development of kinase inhibitor therapy for cancer. *Genes Dev*. 2003 Dec 15;17(24):2998-3010. doi: 10.1101/gad.1152403. PMID: 14701871.
4. Li, Meng-Jiao et al. "Role of gefitinib in the targeted treatment of non-small-cell lung cancer in Chinese patients." *Oncotargets and therapy* vol. 9 1291-302. 9 Mar. 2016, doi:10.2147/OTT.S80635
5. Hurwitz H, Fehrenbacher L, Novotny W, Cartwright T, Hainsworth J, Heim W, Berlin J, Baron A, Griffing S, Holmgren E, Ferrara N, Fyfe G, Rogers B, Ross R, Kabbinavar F. Bevacizumab plus irinotecan, fluorouracil, and leucovorin for metastatic colorectal cancer. *N Engl J Med*. 2004 Jun 3;350(23):2335-42. doi: 10.1056/NEJMoa032691. PMID: 15175435.
6. Sawyers, C., 2004. Targeted cancer therapy. *Nature*, 432(7015), pp.294-297.
7. Engelman, J.A., 2009. Targeting PI3K signalling in cancer: opportunities, challenges and limitations. *Nature Reviews Cancer*, 9(8), pp.550-562.
8. Pardoll, D. The blockade of immune checkpoints in cancer immunotherapy. *Nat Rev Cancer* **12**, 252–264 (2012). <https://doi.org/10.1038/nrc3239>

9. Sharma P, Hu-Lieskovan S, Wargo JA, Ribas A. Primary, Adaptive, and Acquired Resistance to Cancer Immunotherapy. *Cell*. 2017 Feb 9;168(4):707-723. doi: 10.1016/j.cell.2017.01.017. PMID: 28187290; PMCID: PMC5391692.
10. Mahjub, R., Jatana, S., Lee, S.E., Qin, Z., Pauli, G., Soleimani, M., Madadi, S. and Li, S.D., 2018. Recent advances in applying nanotechnologies for cancer immunotherapy. *Journal of controlled release*, 288, pp.239-263.
11. Nishino, Mizuki, et al. "Developing a common language for tumor response to immunotherapy: immune-related response criteria using unidimensional measurements." *Clinical cancer research* 19.14 (2013): 3936-3943.
12. Sung, H, Ferlay, J, Siegel, RL, Laversanne, M, Soerjomataram, I, Jemal, A, Bray, F. Global cancer statistics 2020: GLOBOCAN estimates of incidence and mortality worldwide for 36 cancers in 185 countries. *CA Cancer J Clin*. 2021; 71: 209- 249.
13. Weinberg, R. A., and Douglas Hanahan. "The hallmarks of cancer." *Cell* 100.1 (2000): 57-70.
14. Hanahan, Douglas, and Judah Folkman. "Patterns and emerging mechanisms of the angiogenic switch during tumorigenesis." *cell* 86.3 (1996): 353-364.
15. Berx, Geert, and Frans Van Roy. "Involvement of members of the cadherin superfamily in cancer." *Cold Spring Harbor perspectives in biology* 1.6 (2009): a003129.
16. Vinay, Dass S., et al. "Immune evasion in cancer: Mechanistic basis and therapeutic strategies." *Seminars in cancer biology*. Vol. 35. Academic Press, 2015.

17. Zhang, Jian, Yi Lu, and Kenneth J. Pienta. "Multiple roles of chemokine (CC motif) ligand 2 in promoting prostate cancer growth." *Journal of the National Cancer Institute* 102.8 (2010): 522-528.
18. Gordon, Siamon. "Alternative activation of macrophages." *Nature reviews immunology* 3.1 (2003): 23-35.
19. Chen, Peiwen, et al. "Tumor-associated macrophages promote angiogenesis and melanoma growth via adrenomedullin in a paracrine and autocrine manner." *Clinical cancer research* 17.23 (2011): 7230-7239.
20. Sangaletti, Sabina, et al. "Macrophage-derived SPARC bridges tumor cell-extracellular matrix interactions toward metastasis." *Cancer research* 68.21 (2008): 9050-9059.
21. Noel, Marcus Smith, et al. "Orally administered CCR2 selective inhibitor CCX872-b clinical trial in pancreatic cancer." (2017): 276-276.
22. Scala, Stefania. "Molecular pathways: targeting the CXCR4–CXCL12 axis—untapped potential in the tumor microenvironment." *Clinical cancer research* 21.19 (2015): 4278-4285.
23. Bonapace, Laura, et al. "Cessation of CCL2 inhibition accelerates breast cancer metastasis by promoting angiogenesis." *Nature* 515.7525 (2014): 130-133.
24. Rogers, Thea L., and Ingunn Holen. "Tumour macrophages as potential targets of bisphosphonates." *Journal of translational medicine* 9.1 (2011): 1-17.
25. Pyonteck, Stephanie M., et al. "CSF-1R inhibition alters macrophage polarization and blocks glioma progression." *Nature medicine* 19.10 (2013): 1264-1272.

26. Cannarile, Michael A., et al. "Colony-stimulating factor 1 receptor (CSF1R) inhibitors in cancer therapy." *Journal for immunotherapy of cancer* 5.1 (2017): 1-13.
27. Calvo, Dominica, et al. "CLA-1 is an 85-kD plasma membrane glycoprotein that acts as a high-affinity receptor for both native (HDL, LDL, and VLDL) and modified (OxLDL and AcLDL) lipoproteins." *Arteriosclerosis, thrombosis, and vascular biology* 17.11 (1997): 2341-2349.
28. Gangadhar, Tara C., and Robert H. Vonderheide. "Mitigating the toxic effects of anticancer immunotherapy." *Nature reviews Clinical oncology* 11.2 (2014): 91-99.
29. Calvo, Dominica, et al. "CLA-1 is an 85-kD plasma membrane glycoprotein that acts as a high-affinity receptor for both native (HDL, LDL, and VLDL) and modified (OxLDL and AcLDL) lipoproteins." *Arteriosclerosis, thrombosis, and vascular biology* 17.11 (1997): 2341-2349.
30. Danilo, Christiane, et al. "Scavenger receptor class B type I regulates cellular cholesterol metabolism and cell signaling associated with breast cancer development." *Breast Cancer Research* 15.5 (2013): 1-13.
31. Cormode, David P., et al. "Comparison of synthetic high density lipoprotein (HDL) contrast agents for MR imaging of atherosclerosis." *Bioconjugate chemistry* 20.5 (2009): 937-943.
32. Scheetz, Lindsay M., et al. "Synthetic HDL nanoparticles delivering docetaxel and CpG for chemoimmunotherapy of colon adenocarcinoma." *International journal of molecular sciences* 21.5 (2020): 1777.

33. Van Lenten, Brian J., et al. "Apolipoprotein AI mimetic peptides." *Current atherosclerosis reports* 11.1 (2009): 52-57.